Intermediate-depth earthquake generation and shear zone formation caused by grain size reduction and shear heating

M. Thielmann[1,2]*, A. Rozel[1], B.J.P. Kaus[3], and Y. Ricard[4]
[1]Institut für Geophysik, ETH Zürich, Sonneggstrasse 5, 8092 Zurich, Switzerland
[2]Institute for Building Materials, ETH Zürich, Stefano-Franscini-Platz 3, 8093 Zurich, Switzerland
[3]Institute of Geosciences, Johannes Gutenberg University, Mainz, J.J. Becherweg 21, 55128 Mainz, Germany
[4]Laboratoire de Géologie de Lyon, Ecole Normale Supérieure de Lyon, Université de Lyon-1, CNRS, 69364 Lyon Cedex 07, France

ABSTRACT

The underlying physics of intermediate-depth earthquakes have been an enigmatic topic; several studies support either thermal runaway or dehydration reactions as viable mechanisms for their generation. Here we present fully coupled thermomechanical models that investigate the impact of grain size evolution and energy feedbacks on shear zone and pseudotachylite formation. Our results indicate that grain size reduction weakens the rock prior to thermal runaway and significantly decreases the critical stress needed for thermal runaway, making it more likely to result in intermediate-depth earthquakes at shallower depths. Furthermore, grain size is reduced in and around the shear zone, which agrees with field and laboratory observations where pseudotachylites are embedded in a simultaneously formed mylonite matrix. The decrease in critical stress to initialize localization has important implications for large-scale geodynamics, as this mechanism might induce lithosphere-scale shear zones and subduction initiation. We suggest that the combination of grain size reduction and shear heating explains both the occurrence of intermediate-depth earthquakes and the formation of large-scale shear zones.

INTRODUCTION

Intermediate-depth earthquakes occur in the subducting lithosphere at depths between 50 and 300 km. Their origin is puzzling because the pressures at those depths require very high differential stresses, which are unlikely to be reached because ductile mechanisms should govern deformation at those temperatures. Two main mechanisms have been proposed to trigger intermediate-depth earthquakes: dehydration embrittlement and thermal runaway. Dehydration embrittlement (e.g., Hacker et al., 2003; Frohlich, 2006) results from increased pore pressures due to fluids released in metamorphic reactions, thus facilitating brittle failure.

Thermal runaway results from the feedback between weakening due to shear heating and the temperature-dependent rock rheology (e.g., Kelemen and Hirth, 2007; Andersen et al., 2008; John et al., 2009; Braeck and Podladchikov, 2007; Thielmann and Kaus, 2012). Hobbs et al. (1986) and Ogawa (1987) proposed that, with a viscoelastic rheology, this process could result in intermediate-depth and deep earthquakes. Evidence for thermal runaway can be found in the field in the form of pseudotachylites (e.g., Andersen et al., 2008). Although many of them are associated with melting due to frictional heating during brittle failure, some are found in settings where ductile thermal runaway is the most plausible explanation (e.g., Ueda et al., 2008). Numerical models show that this mechanism requires large differential stresses (e.g., John et al., 2009). Analyses of ultramafic pseudotachylites in Corsica suggest that released elastic stresses are as high as 580 MPa (Andersen et al., 2008). Other studies suggest that shear heating could result in decomposition and elevated pore pressures (Poulet et al., 2014).

A possible mechanism for weakening prior to thermal runaway is grain size reduction, which might significantly affect shear zone evolution (Kameyama and Yuen, 1997). Evidence for the simultaneous formation of ultramylonites and pseudotachylites has been found in the laboratory (Kim et al., 2010) and the field (see Deseta et al., 2014, and references therein). Here we investigate the effect of grain size evolution on thermal runaway in the ductile regime.

RHEOLOGY, GRAIN SIZE EVOLUTION, AND VISCOUS HEATING

We employ a Maxwell viscoelastic rheology with a viscous rheology composed of two deformation mechanisms: diffusion and dislocation creep. We consider an infinite slab of thickness L, which is deformed in the x direction with a constant background strain rate $\dot{\varepsilon}_{BG}$. The total shear strain rate $\dot{\varepsilon}(y)$ is then given by

$$\dot{\varepsilon} = \underbrace{\frac{1}{G}\frac{\partial \tau}{\partial t}}_{\substack{\text{elastic}\\ \text{strain rate}}} + \underbrace{\dot{\varepsilon}_{dif} + \dot{\varepsilon}_{dis}}_{\substack{\text{viscous}\\ \text{strain rate}}}, \quad (1)$$

where $\dot{\varepsilon}_{dif}(y)$ and $\dot{\varepsilon}_{dis}(y)$ are diffusion and dislocation creep strain rate, respectively, G is the shear modulus, and $\partial\tau/\partial t$ is the time derivative of the uniform shear stress (see the GSA Data Repository[1] for details). Depending on stress, temperature, and grain size, one deformation mechanism is dominant, with only diffusion creep being grain size sensitive. Diffusion creep dominates at small grain sizes and stresses; dislocation creep prevails at large stresses and grain sizes (see Fig. 1).

We model grain size evolution with an evolution law based on first principles (Ricard and Bercovici, 2009; Rozel et al., 2011) and consider the whole grain size distribution (i.e., in a microscopic volume, larger grains can undergo dislocation creep while smaller grains deform by diffusion). In this model, grain size reduction results in an increase of total grain boundary surface area; this requires energy. The average grain size evolution is described as a combination of grain growth and grain size reduction. Reduction is driven by the dissipation of a fraction of the deformational work in the dislocation creep regime:

$$\frac{\partial R}{\partial t} = \frac{G}{pR^{p-1}} - \frac{f_0 F_R}{\gamma} R^2 \tau \dot{\varepsilon}_{dis}, \quad (2)$$

where R is the average grain size, $G = k_0\, e^{-Q_g/RT}$ is a temperature-dependent growth term, p is the growth exponent, γ is the surface tension, and F_R is a constant factor depending on the characteristics of the grain size distribution (see the Data Repository). The first term on the right side of Equation 2 describes normal grain growth (Hillert, 1965); the second term describes grain size reduction by recrystallization. The partition of deformational work that results in grain size reduction is governed by the parameter $0 \le f_0 \le 1$ (lambda factor of Austin and Evans, 2007), which is likely both strain and temperature dependent (Chrysochoos and Belmahjoub, 1992; Rozel et al., 2011). Grain growth in single-phase rocks is fast (Karato, 1989), but can be significantly decelerated in the presence of secondary phases (e.g.,

*E-mail: thielmann.marcel@gmail.com

[1]GSA Data Repository item 2015270, derivation of governing equations, description of the numerical method, listing of material parameters, and additional results, is available online at www.geosociety.org/pubs/ft2015.htm, or on request from editing@geosociety.org or Documents Secretary, GSA, P.O. Box 9140, Boulder, CO 80301, USA.

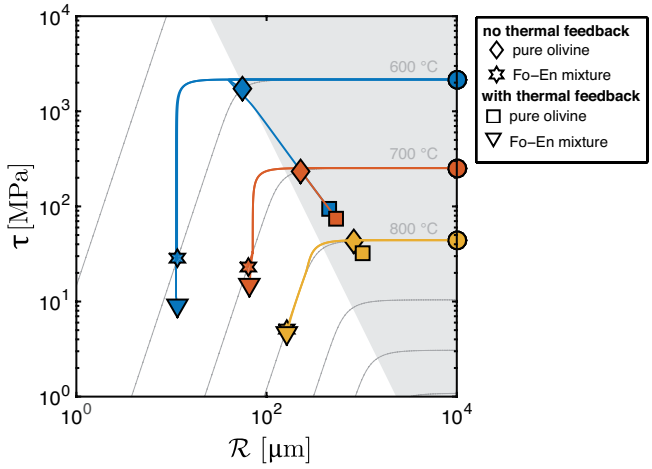

Figure 1. Stress and grain size evolution (*R* = average grain size) of an adiabatic and spatially homogeneous model underlain by a deformation mechanism map for dry olivine (Hirth and Kohlstedt, 2003) for a constant background strain rate $\dot{\varepsilon} = 10^{-15}$ s^{-1}. Only dislocation (grain size insensitive) and diffusion (grain size sensitive) creep are considered. Thin gray lines denote the viscous (steady state) strength of olivine for a given grain size and temperature. In the shaded region, dislocation creep is dominant. Colored lines and symbols denote the stress and grain size evolution of viscoelastic simulations; initial conditions are denoted by circles (temperature can vary along those lines). Different symbols denote different simulation scenarios (see text). Fo-En—forsterite-enstatite.

Faul and Scott, 2006; Hiraga et al., 2010; Herwegh et al., 2011; Bercovici and Ricard, 2012, 2014; Tasaka and Hiraga, 2013; Linckens et al., 2015).

Shear heating is the conversion of deformational work to heat and represents a source term in the temperature equation (see the Data Repository):

$$\frac{\partial T}{\partial t} = \kappa \frac{\partial T^2}{\partial x^2} + \left(1 - f_0\right)\frac{\tau \dot{\varepsilon}_{dis}}{\rho c} + \frac{\tau \dot{\varepsilon}_{dif}}{\rho c} + \frac{\gamma G}{\rho c p F_R R^{p+1}}, \quad (3)$$

where the change in temperature, T, depends on thermal diffusion (with diffusivity κ), shear heating, and grain size evolution (ρ is density, c is heat capacity). The deformational work available for viscous heating is the total irreversible deformational work $\tau(\dot{\varepsilon}_{dis} + \dot{\varepsilon}_{dif})$ minus the work used for grain size reduction, $f_0 \tau \dot{\varepsilon}_{dis}$. In addition, grain boundary energy is converted to heat during grain growth (last term in Equation 3). Shear heating and grain size reduction result in weakening, but it is unclear which mechanism is more effective in the deeper lithosphere. Elevated temperatures result in faster grain growth, and thus in hardening rather than weakening. Conversely, higher temperatures result in weaker rocks. Due to the highly nonlinear nature of both mechanisms, it is therefore necessary to investigate their interplay in more detail.

INFLUENCE OF GRAIN GROWTH PARAMETERS AND SHEAR HEATING ON WEAKENING

The deformation mechanism map for dry olivine (Hirth and Kohlstedt, 2003) is shown in Figure 1 (only diffusion and dislocation creep are considered; gray lines are computed for a strain rate of 10^{-15} s^{-1} and different temperatures) together with the results from 12 adiabatic and spatially homogeneous viscoelastic simulations. We tested four different scenarios: (1) pure olivine grain growth, no thermal feedback; (2) grain growth of a forsterite-enstatite (Fo-En) mixture, no thermal feedback; (3) pure olivine grain growth and thermal feedback; and (4) Fo-En mixture and thermal feedback. We solve Equations 1–3 for a medium submitted to a uniform strain rate with an implicit adaptive time stepping scheme (see the Data Repository), which allows us to use very small time steps when necessary (e.g., during thermal runaway the step size becomes as small as 2 ms). Initial conditions (circles) are the steady-state stress for the initial grain size (1 cm) and temperature (600, 700, and 800 °C). The simulation is stopped at time t, when a shear strain of $\dot{\varepsilon}_{BG} t = 2$ has been reached. Grain growth parameters as well as shear heating do not have a strong influence on early stress evolution, but affect later stages (in Fig. 1, the lines are on top of each other early on before diverging later).

If grain growth parameters of Karato (1989) are used (pure olivine), weakening due to grain size reduction is almost negligible (diamonds, Fig. 1), but it is stronger if shear heating is active (squares, Fig. 1). As grain size is simultaneously increasing, the decrease in strength is attributed to the temperature increase caused by shear heating (most effective at low temperatures and hence high stresses). When grain growth parameters of an Fo-En mixture are employed (Hiraga et al., 2010; Tasaka and Hiraga, 2013), grain size is considerably reduced and significant weakening occurs (stars when the simulations are performed at constant temperature, triangles with thermal feedback; Fig. 1). This is due to the released elastic energy that results in a nonnegligible amount of deformational work done in dislocation creep, although the material is mainly deforming in diffusion creep. Shear heating amplifies weakening in those cases, indicating a positive feedback between both mechanisms (which decreases for increasing background temperatures). These examples demonstrate that the interplay between elasticity, grain size evolution, and shear heating is not straightforward and that more complex models are needed to unravel their mutual feedbacks.

SIMULTANEOUS FORMATION OF PSEUDOTACHYLITE AND ULTRAMYLONITE DURING THERMAL RUNAWAY

Due to the assumptions, the previous model cannot be used to model the formation of localized shear zones where melting, and thus the formation of pseudotachylites, takes place. We therefore simulate the deformation of a heterogeneous nonadiabatic slab of width L = 100 km under simple shear.

We solve the system of equations with a finite difference method (see the Data Repository). In the model center, a material perturbation with width h = 100 m was introduced. Here the rheological prefactors of the creep laws were increased by 1% (some heterogeneity is required to initiate localization). The initial average grain size is set to 1 cm and the initial stress is zero. Background strain rates and initial temperatures were varied between 10^{-15} and 10^{-10} s^{-1} and 500 and 1000 °C. The spatial resolution varied from 10 cm in the perturbed zone to 1 km toward the domain boundaries. In the center of the perturbed zone (from –20 to 20 m), resolution was kept at 10 cm. The maximum temperature is limited to 1900 K, as melting and other chemical reactions would occur even before reaching this temperature (e.g., Veveakis et al., 2010). The validity of our models is thus limited to stages before such temperatures are reached and later stages can only be interpreted qualitatively.

We test the same four scenarios (grain growth parameters are only varied in the perturbed zone; the surrounding matrix always consists of pure olivine). Due to the lack of (1) a physical description of the evolution of f_0, and (2) the lack of experimental data, we chose a constant value $f_0 = 0.1$ (i.e., 10% of the deformational work is used for recrystallization). We also ran simulations where a larger value of f_0 was used (0.5) and results did not change significantly (see the Data Repository), although transient stages are affected (see also Herwegh et al., 2014).

The temporal evolution of stress, grain size, and temperature at a strain rate of 5×10^{-15} s^{-1} and a background temperature of 900 K is shown in Figures 2A–2C. The degree of localization can be measured by the ratio between the strain rate in the shear zone center (z = 0) to $\dot{\varepsilon}_{BG}$ (Fig. 2D). In simulations without thermal feedback, we observe an initial period of stress build-up (elastic loading) until stresses and grain sizes reach a steady state. The steady-state stress is approximately twice as large if growth parameters of pure olivine are employed, which stems from the larger equilibrium grain size. In Figures 2E and 2F, we show cross sections of displacement and grain size at various times (filled circles in Figs. 2A–2D) of

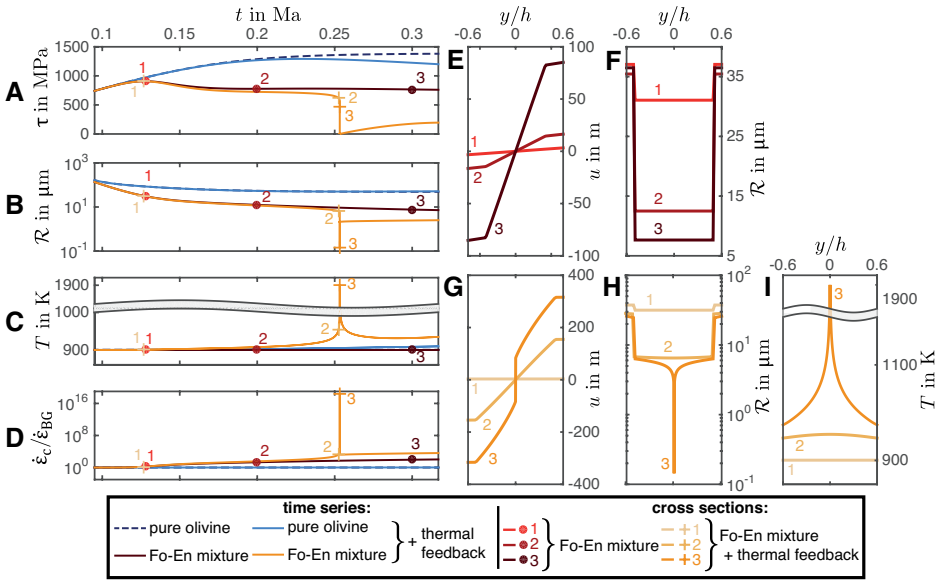

Figure 2. Example simulations (spatially heterogeneous) with an initial temperature of 900 K and a background strain rate of 5 × 10^{-15} s^{-1}. A–D: Time (*t*) series of stress (τ), grain size (*R*), temperature (*T*), and strain rate normalized with the background strain rate ($\dot{\varepsilon}_c/\dot{\varepsilon}_{BG}$; the latter three are all taken at the center of the model). E, F: Cross sections of displacement (*u*) and grain size, respectively, at different times (filled circles in A–D) for a simulation with a forsterite-enstatite (Fo-En) mixture in the perturbed zone (no thermal feedback). G–I: Cross sections of displacement, grain size, and temperature at different times (crosses in A–D) for a simulation with an Fo-En mixture and thermal feedback.

the Fo-En mixture simulation without thermal feedback between –0.6 and 0.6 *h* (*h* is the width of the perturbed zone). At later stages, grain size is decreased in the perturbed zone. Strain rates are elevated inside this zone, which is more deformed than the surrounding matrix (Fig. 2F).

The two simulations with thermal feedback show a different behavior: in the case of pure olivine, a similar maximum stress is reached as in the case without thermal feedback, but the material is subsequently weakened due to increasing temperature. The system is still stable (no occurrence of thermal runaway). In the case of the Fo-En mixture, however, the behavior changes drastically. In the beginning, stress behaves similarly, as in the case without thermal feedback. However, at ca. 0.25 Ma a sudden stress drop occurs. This event can also be seen in the other quantities. Due to the quasi-instantaneous release of elastic energy, temperature increases (until it saturates at the cutoff value) and grain size decreases significantly.

In Figures 2G–2I, cross sections of displacement, grain size, and temperature of the Fo-En mixture simulation with thermal feedback are shown (corresponding times are denoted as crosses in Figs. 2A–2D). Upon thermal runaway we observe self-localization in the central part of the perturbed zone; this can be attributed to a significant temperature increase and a drastic grain size decrease. The high temperatures would certainly result in melting and thus pseudotachylite formation, which is embedded in an ultramylonite matrix. Because we do not include the effects of melting in our model, we cannot make precise predictions about the further shear zone evolution.

Grain size starts to decrease (thus weakening the rock) prior to the actual thermal runaway event. This is in agreement with observations of Kim et al. (2010) and Deseta et al. (2014), although the formation of pseudotachylites was related to prior brittle failure and frictional heating in the first study. In titanium alloys, dynamic recrystallization was found to precede and trigger thermal runaway without prior brittle failure (Rittel et al., 2008). Hence grain size evolution assists thermal runaway as it amplifies the effect of small temperature perturbations through a reduced grain size and significantly reduces the critical stress needed for thermal runaway.

CRITICAL STRESS NEEDED FOR THERMAL RUNAWAY

Kelemen and Hirth (2007) and John et al. (2009) demonstrated that shear heating is a viable mechanism for intermediate-depth earthquake generation. However, the critical stress in their studies at depths of ~80 km was relatively large (~1 GPa or larger). The simulations shown in Figure 2 indicate that the critical stresses needed for thermal runaway are reduced to significantly smaller values if grain growth is hindered by secondary phases. We therefore analyzed the spatially heterogeneous simulations for the two scenarios, where grain size evolution and shear heating are both active, to determine (1) the maximum stress, and (2) whether thermal runaway occurs. The results of this analysis are shown in Figure 3, where the maximum stress is plotted as a function of background strain rate and background temperature. The 600 MPa isoline is plotted as a solid white line; a red line indicates the boundary between stable and runaway regimes (Fig. 3). It can be seen that grain size evolution significantly reduces the critical stress needed for thermal runaway. Note that thermal runaway also occurs for fast grain growth, but only at larger stresses.

IMPLICATIONS ON THE OCCURRENCE OF INTERMEDIATE-DEPTH EARTHQUAKES AND DUCTILE SHEAR ZONES

The models presented here agree with previous suggestions that thermal runaway is a viable mechanism for the generation of intermediate-depth earthquakes. However, they indicate that the stresses required for thermal runaway are significantly lower when grain size evolution is considered, which makes thermal runaway an even stronger candidate to generate intermediate depth earthquakes. For secondary-phase inhibited

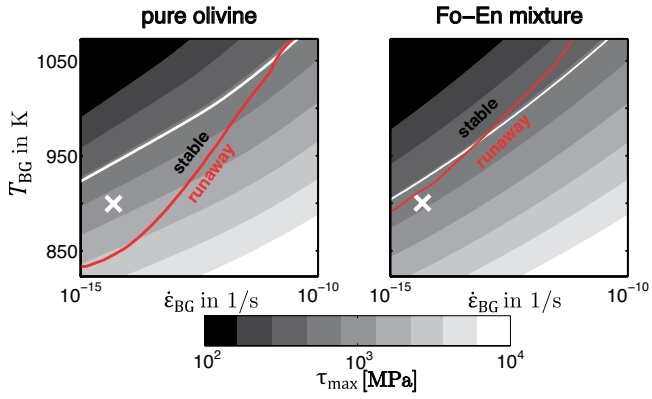

Figure 3. Occurrence of thermal runaway for different scenarios and corresponding stresses. Background colors denote the maximum stress reached in each simulation. The white line is the 600 MPa isocontour and the red line denotes the regime boundary between stable and unstable regimes (where thermal runaway occurs). Crosses indicate conditions of the experiments shown in Figure 2. T_{BG}—background temperature; $\dot{\varepsilon}_{BG}$—background strain rate; τ—stress.

grain growth, the critical stress for thermal runaway is, e.g., ~700 MPa at 890 K (at a strain rate of 10^{-15} s^{-1}), which corresponds to a depth of ~60 km if a thermal gradient of 10 °C/km is assumed. This agrees with the findings of Linckens et al. (2015) that localization at these temperatures and depths only takes place in polymineralic olivine-pyroxene mixtures. At shallower depths the critical stress exceeds the brittle strength of rocks such that ductile failure is not likely. However, due to frictional heating, ductile deformation can also set in at later stages (Hirose and Shimamoto, 2005), even without producing pseudotachylites (Smith et al., 2013).

The stress drops observed in our models are several hundred megapascals. Stress drops of this magnitude have been observed in field studies of pseudotachylites (580 MPa; Andersen et al., 2008) and intermediate-depth earthquakes (100 MPa; Prieto et al., 2013).

As can be seen from Figure 3, thermal runaway events occur most readily at high temperatures and large strain rates; e.g., the lowest critical stress needed for thermal runaway at a temperature of 1073 K and a background strain rate of 10^{-11} s^{-1} is ~400 MPa. Such strain rates could be reached if a shallower (brittle) earthquake loads deeper parts of the lithosphere where brittle failure is less likely to occur. Ductile failure due to thermal runaway may be initiated as a continuation of the shallower earthquake, thus resulting in larger rupture planes and more energy release.

ACKNOWLEDGMENTS

We thank T.B. Anderson, M. Herwegh, L. Montési, and an anonymous reviewer for their constructive reviews. The research leading to these results received funding from Crystal2Plate, an FP7 funded Marie Curie Action under grant agreement PITN-GA-2008- 215353. Thielmann received support from SNSF grant 200021-143299, Rozel was supported by European Research Council (ERC) project iGEO, and Kaus was supported by ERC starting grant 258830.

REFERENCES CITED

Andersen, T.B., Mair, K., Austrheim, H., Podladchikov, Y.Y., and Vrijmoed, J.C., 2008, Stress release in exhumed intermediate and deep earthquakes determined from ultramafic pseudotachylyte: Geology, v. 36, p. 995–998, doi:10.1130/G25230A.1.

Austin, N., and Evans, B., 2007, Paleowattmeters: A scaling relation for dynamically recrystallized grain size: Geology, v. 35, p. 343–346, doi:10.1130/G23244A.1.

Bercovici, D., and Ricard, Y., 2012, Mechanisms for the generation of plate tectonics by two-phase grain-damage and pinning: Physics of the Earth and Planetary Interiors, v. 202–203, p. 27–55, doi:10.1016/j.pepi.2012.05.003.

Bercovici, D., and Ricard, Y., 2014, Plate tectonics, damage and inheritance: Nature, v. 508, p. 513–516, doi:10.1038/nature13072.

Braeck, S., and Podladchikov, Y.Y., 2007, Spontaneous thermal runaway as an ultimate failure mechanism of materials: Physical Review Letters, v. 98, 095504, doi:10.1103/PhysRevLett.98.095504.

Chrysochoos, A., and Belmahjoub, F., 1992, Thermographic analysis of thermomechanical couplings: Archives of Mechanics, v. 44, p. 55–68.

Deseta, N., Andersen, T.B., and Ashwal, L.D., 2014, A weakening mechanism for intermediate-depth seismicity? Detailed petrographic and microtextural observations from blueschist facies pseudotachylytes, Cape Corse, Corsica: Tectonophysics, v. 610, p. 138–149, doi:10.1016/j.tecto.2013.11.007.

Faul, U.H., and Scott, D., 2006, Grain growth in partially molten olivine aggregates: Contributions to Mineralogy and Petrology, v. 151, p. 101–111, doi:10.1007/s00410-005-0048-1.

Frohlich, C., 2006, Deep earthquakes: Cambridge, UK, Cambridge University Press, 588 p.

Hacker, B., Peacock, S., Abers, G., and Holloway, S., 2003, Subduction factory 2. Are intermediate-depth earthquakes in subducting slabs linked to metamorphic dehydration reactions: Journal of Geophysical Research, v. 108, no. B1, 2030, doi:10.1029/2001JB001129.

Herwegh, M., Linckens, J., Ebert, A., Berger, A., and Brodhag, S., 2011, The role of second phases for controlling microstructural evolution in polymineralic rocks: A review: Journal of Structural Geology, v. 33, p. 1728–1750, doi:10.1016/j.jsg.2011.08.011.

Herwegh, M., Poulet, T., Karrech, A., and Regenauer-Lieb, K., 2014, From transient to steady state deformation and grain size: A thermodynamic approach using elasto-visco-plastic numerical modeling: Journal of Geophysical Research, v. 119, p. 900–918, doi:10.1002/2013JB010701.

Hillert, M., 1965, On theory of normal and abnormal grain growth: Acta Metallurgica, v. 13, p. 227–238, doi:10.1016/0001-6160(65)90200-2.

Hiraga, T., Tachibana, C., Ohashi, N., and Sano, S., 2010, Grain growth systematics for forsterite ± enstatite aggregates: Effect of lithology on grain size in the upper mantle: Earth and Planetary Science Letters, v. 291, p. 10–20, doi:10.1016/j.epsl.2009.12.026.

Hirose, T., and Shimamoto, T., 2005, Growth of molten zone as a mechanism of slip weakening of simulated faults in gabbro during frictional melting: Journal of Geophysical Research, v. 110, B05202, doi:10.1029/2004JB003207.

Hirth, G., and Kohlstedt, D.L., 2003, Rheology of the upper mantle and the mantle wedge: A view from the experimentalists, *in* Eiler, J., ed., Inside the subduction factory: American Geophysical Union Geophysical Monograph 138, p. 83–105, doi:10.1029/138GM06.

Hobbs, B.E., Ord, A., and Teyssier, C., 1986, Earthquakes in the ductile regime: Pure and Applied Geophysics, v. 124, p. 309–336, doi:10.1007/BF00875730.

John, T., Medvedev, S., Rüpke, L., and Andersen, T., 2009, Generation of intermediate-depth earthquakes by self-localizing thermal runaway: Nature Geoscience, v. 2, p. 137–140, doi:10.1038/ngeo419.

Kameyama, M., and Yuen, D., 1997, The interaction of viscous heating with grain-size dependent rheology in the formation of localized slip zones: Geophysical Research Letters, v. 24, p. 2523–2526, doi:10.1029/97GL02648.

Karato, S.-I., 1989, Grain growth kinetics in olivine aggregates: Tectonophysics, v. 168, p. 255–273, doi:10.1016/0040-1951(89)90221-7.

Kelemen, P., and Hirth, G., 2007, A periodic shear-heating mechanism for intermediate-depth earthquakes in the mantle: Nature, v. 446, p. 787–790, doi:10.1038/nature05717.

Kim, J.-W., Ree, J.-H., Han, R., and Shimamoto, T., 2010, Experimental evidence for the simultaneous formation of pseudotachylyte and mylonite in the brittle regime: Geology, v. 38, p. 1143–1146, doi:10.1130/G31593.1.

Linckens, J., Herwegh, M., and Müntener, O., 2015, Small quantity but large effect—How minor phases control strain localization in upper mantle shear zones: Tectonophysics, v. 643, p. 26–43, doi:10.1016/j.tecto.2014.12.008.

Ogawa, M., 1987, Shear instability in a viscoelastic material as the cause of deep focus earthquakes: Journal of Geophysical Research, v. 92, p. 13,801–13,810, doi:10.1029/JB092iB13p13801.

Poulet, T., Veveakis, M., Regenauer-Lieb, K., and Yuen, D.A., 2014, Thermo-poromechanics of chemically active creeping faults: 3. The role of serpentinite in episodic tremor and slip sequences, and transition to chaos: Journal of Geophysical Research, v. 119, p. 4606–4625, doi:10.1002/2014JB011004.

Prieto, G.A., Florez, M., and Barrett, S.A., 2013, Seismic evidence for thermal runaway during intermediate-depth earthquake rupture: Geophysical Research Letters, v. 40, p. 6064–6068, doi:10.1002/2013GL058109.

Ricard, Y., and Bercovici, D., 2009, A continuum theory of grain size evolution and damage: Journal of Geophysical Research, v. 114, B01204, doi:10.1029/2007JB005491.

Rittel, D., Landau, P., and Venkert, A., 2008, Dynamic recrystallization as a potential cause for adiabatic shear failure: Physical Review Letters, v. 101, 165501, doi:10.1103/PhysRevLett.101.165501.

Rozel, A., Ricard, Y., and Bercovici, D., 2011, A thermodynamically self-consistent damage equation for grain size evolution during dynamic recrystallization: Geophysical Journal International, v. 184, p. 719–728, doi:10.1111/j.1365-246X.2010.04875.x.

Smith, S.A.F., Di Toro, G., Kim, S., Ree, J.-H., Nielsen, S., Billi, A., and Spiess, R., 2013, Coseismic recrystallization during shallow earthquake slip: Geology, v. 41, p. 63–66, doi:10.1130/G33588.1.

Tasaka, M., and Hiraga, T., 2013, Influence of mineral fraction on the rheological properties of forsterite + enstatite during grain-size-sensitive creep: 1. Grain size and grain growth laws: Journal of Geophysical Research, v. 118, p. 3970–3990, doi:10.1002/jgrb.50285.

Thielmann, M., and Kaus, B.J.P., 2012, Shear heating induced lithospheric-scale localization: Does it result in subduction?: Earth and Planetary Science Letters, v. 359–360, p. 1–13, doi:10.1016/j.epsl.2012.10.002.

Ueda, T., Obata, M., Di Toro, G., Kanagawa, K., and Ozawa, K., 2008, Mantle earthquakes frozen in mylonitized ultramafic pseudotachylytes of spinel-lherzolite facies: Geology, v. 36, p. 607–610, doi:10.1130/G24739A.1.

Veveakis, E., Alevizos, S., and Vardoulakis, I., 2010, Chemical reaction capping of thermal instabilities during shear of frictional faults: Journal of the Mechanics and Physics of Solids, v. 58, p. 1175–1194, doi:10.1016/j.jmps.2010.06.010.

Manuscript received 7 April 2015
Revised manuscript received 24 June 2015
Manuscript accepted 26 June 2015

Printed in USA